Ex vivo imaging and quantification of liver fibrosis using second-harmonic generation microscopy

Tzu-Lin Sun[*]
Yuan Liu[*]
Ming-Chin Sung
National Taiwan University
Department of Physics
Taipei, 10617 Taiwan

Hsiao-Ching Chen
National Taiwan University Hospital
Department of Internal Medicine
Taipei, 100 Taiwan
    and
National Taiwan University
College of Medicine
Taipei, 100 Taiwan

Chun-Hui Yang
Vladimir Hovhannisyan
National Taiwan University
Department of Physics
Taipei, 10617 Taiwan

Wei-Chou Lin
Yung-Ming Jeng
National Taiwan University Hospital
    and
National Taiwan University
College of Medicine
Department of Pathology
Taipei, 10002 Taiwan

Wei-Liang Chen
National Taiwan University
Department of Physics
Taipei, 10617 Taiwan

Ling-Ling Chiou
Guan-Tarn Huang
National Taiwan University Hospital
Department of Internal Medicine
Taipei, 100 Taiwan
    and
National Taiwan University
College of Medicine
Taipei, 100 Taiwan

Ki-Hean Kim
Peter T. C. So
Massachusetts Institute of Technology
Department of Mechanical Engineering
    and
Division of Bioengineering
Cambridge, Massachusetts 02139

Yang-Fang Chen
National Taiwan University
Department of Physics
Taipei, 10617 Taiwan

Hsuan-Shu Lee[†]
National Taiwan University
Institute of Biotechnology
    and
National Taiwan University Hospital
Department of Internal Medicine
    and
National Taiwan University
College of Medicine
Taipei, 100 Taiwan

Chen-Yuan Dong[†]
National Taiwan University
Department of Physics
    and
Center for Quantum Science and Engineering
    and
Division of Genomic Medicine
Research Center for Medical Excellence
Biomedical Molecular Imaging Core
Taipei, 100 Taiwan

Abstract. Conventionally, liver fibrosis is diagnosed using histopathological techniques. The traditional method is time-consuming in that the specimen preparation procedure requires sample fixation, slicing, and labeling. Our goal is to apply multiphoton microscopy to efficiently image and quantitatively analyze liver fibrosis specimens bypassing steps required in histological preparation. In this work, the combined imaging modality of multiphoton autofluorescence (MAF) and second-harmonic generation (SHG) was used for the qualitative imaging of liver fibrosis of different METAVIR grades under label-free, *ex vivo* conditions. We found that while MAF is effective in identifying cellular architecture in the liver specimens, it is the spectrally distinct SHG signal that allows the characterization of the extent of fibrosis. We found that qualitative SHG imaging can be used for the effective identification of the associated features of liver fibrosis specimens graded METAVIR 0 to 4. In addition, we attempted to associate quantitative SHG signal to the different METAVIR grades and found that an objective determination of the extent of disease progression can be made. Our approach demonstrates the potential of using multiphoton imaging in rapid classification of *ex vivo* liver fibrosis in the clinical setting and investigation of liver fibrosis–associated physiopathology in animal models *in vivo*. © *2010 Society of Photo-Optical Instrumentation Engineers.* [DOI: 10.1117/1.3427146]

1 Introduction

Conventional histopathology is regarded as the gold standard in diagnosing tissue pathologies such as liver fibrosis. In this

[*]These authors contributed equally to this work.
[†]Address all correspondence to: Chen-Yuan Dong, Tel: 886-2-3366-5155; Fax: 886-2-2363-9984; E-mail: cydong@phys.ntu.edu.tw and Hsuan-Shu Lee, Tel: 886-2-3366-6007; Fax: 886-2-3366-6001; E-mail: benlee@ntu.edu.tw.

approach, sample preparation procedures are time-consuming in that the specimens required fixation, sectioning, and labeling. In histopathological examination, the extent of liver fibrosis is examined by experienced pathologists using biopsy specimens. Frequently, the METAVIR scoring system is used for the semiquantitative determination of biopsied liver fibrosis specimens. This system classifies liver fibrosis into five categories (grades 0 to 4) according to the morphological features of collagen fiber formation within the biopsied specimens. Specifically, the key morphological features of no fibrosis, portal fibrosis without septa, fibrosis with few septa, numerous septa without cirrhosis, and cirrhosis are respectively associated with METAVIR scores of 0 to 4 Ref. [1]. While the METAVIR system is heavily used in the clinical setting, the qualitative nature of the grading process prevents a more precise and quantitative determination of the extent of liver fibrosis to be achieved. Furthermore, the histopathological method is limiting in that the sample preparation procedures can be time-consuming and in that this approach prevents subsequent tissue dynamics to be followed *in vivo*.

In recent years, multiphoton microscopy emerged as a promising technique for the qualitative imaging and quantitative characterization of many tissues. Key advantages such as high axial-depth discrimination, reduced photodamage, and enhanced penetration depths enable this technique to be the preferred tool for minimally invasive imaging.[2,3] In addition to fluorescence excitation, the nonlinear polarization effect of second-harmonic generation (SHG) has also been demonstrated to be useful for imaging and characterizing abnormalities of the extracellular collagen matrix.[4–8]

To understand the SHG phenomenon, consider the polarization $\widetilde{P}(t)$ of a material that depends on the susceptibility tensor χ and is a polynomial function of the applied external electric field $\widetilde{E}(t)$:

$$\widetilde{P}(t) = \varepsilon_0[\chi^{(1)}\widetilde{E}(t) + \chi^{(2)}\widetilde{E}^2(t) + \chi^{(3)}\widetilde{E}^3(t) + \cdots]. \quad (1)$$

In the case of collagen fibers, the inherent noncentrosymmetric structure gives rise to a nonvanishing second-order susceptibility tensor $\chi^{(2)}$ that, when coupled to the external electric field, generates a nonlinear optical signal at exactly half the wavelength of the excitation source. Second-harmonic generation (SHG) signal has been demonstrated to be effective for the label-free (*in vivo* or *ex vivo*) imaging of tissues such as collagen and muscle fibers.[5,9–11] For pathological studies, earlier studies have demonstrated that multiphoton autofluorescence (MAF) and SHG imaging are effective in diagnosing pathological tissues such as skin aging, basal cell carcinoma, keratoconus, atherosclerosis, *osteogenesis imperfecta*, and muscular diseases.[6,7,12–17]

Similar studies have been performed for the diagnosis of liver fibrosis, in a forward SHG detection configuration.[5,18] To further demonstrate the clinical potential of such a method, we investigated frozen sections of human liver fibrosis tissues using backward-detected MAF and SHG signal. The ability for *in vivo* liver imaging using such a backward-detection setup has been demonstrated in our previous work.[19–21] In addition, the use of human tissue allows us to compare the quantitative analysis of the acquired images with the METAVIR scoring system of human liver fibrosis specimens.

Our aim is to show that the intrinsic multiphoton signatures from the tissue specimens can identify features useful for the qualitative evaluation of disease progression and to provide a quantitative link between the SHG signal and liver fibrosis tissues of different METAVIR grades.

2 Materials and Methods

2.1 Multiphoton Imaging System

The multiphoton imaging microscope used in this study is similar to one previously described.[22] In short, the 780-nm output of a femtosecond, titanium-sapphire laser (Tsunami, Spectra Physics, Mountain View, California) pumped by a diode-pumped, solid-state laser (Millennia X, Spectra Physics) was used for excitation. The excitation source was guided toward a modified upright microscope (E800, Nikon, Tokyo, Japan) by a set of *x*-*y* galvanometer-driven, scanning mirrors (model number 6210, Cambridge Technology, Cambridge, Massachusetts). Upon entering the microscope, the laser was beam-expanded to ensure overfilling of the objective's back aperture. The expanded laser beam is reflected into the high numerical aperture focusing objective by the main dichroic mirror (435DCXR, Chroma Technology, Rockingham, Vermont). For high-resolution imaging, a high-numerical-aperture, oil-immersion objective (Nikon S Fluor 40×/NA 1.3) was used. Otherwise, an oil-immersion objective (Nikon Plan Fluor 20×/NA 0.75 MI) was used to acquire large-area images for SHG signal quantification. The MAF and SHG signals produced at the focal spot were collected in the epi-illuminated geometry and separated by a secondary dichroic and additional bandpass filters (E435LP 700SP, HQ 390/20, Chroma Technology) for the collection and isolation of broadband autofluorescence (435 to 700 nm) and SHG (380 to 400 nm) signals, respectively. Single-photon counting photomultiplier tubes (R7400P, Hamamatsu, Hamamatsu City, Japan) and home-built discriminators were used for the detection and processing of the signal photons. For the acquisition of large-area, multiphoton images, a sample translation stage (H101, Prior Scientific, Cambridge, UK) was used to translate the specimen after each small-area optical scan. The individual small images 110×110 μm^2 in area (S Fluor 40 × objective, Nikon) and 220×220 μm^2 in area (Plan Fluor 20× objective, Nikon) are then assembled to form a large-area image 1980×1540 μm^2 (S Fluor 40× objective) for qualitative multiphoton imaging and 3300×3300 μm^2 (Plan Fluor 20× objective) for quantitative SHG measurement. In this manner, high resolution, large-area view, and quantification of the severity of the tissue fibrosis can be achieved.

2.2 Preparation of Frozen Specimens

In order to demonstrate the imaging capabilities of multiphoton microscopy in label-free imaging of liver fibrosis specimens, frozen tissues were used. One tissue block from each patient was frozen at $-80\,°$C after embedding with optical cutting temperature compound. Each frozen tissue block was sectioned into specimens approximately 10 μm in thickness. One of two adjacent sections was used for multiphoton imaging and the other sample was stained with Masson's trichrome labeling for collagen-specific, histological comparison to the multiphoton results. In addition, since the intensity profile of

the multiphoton signals was not uniform across the imaged area, multiphoton images of the liver fibrosis specimens were corrected using an image field flatness correction algorithm developed in our laboratory.[23]

2.3 Label-Free Optical Biopsy and Quantification of Liver Fibrosis

Following preparation of the liver fibrosis specimens as described earlier, we performed MAF and SHG imaging of liver fibrosis specimens that have been histologically graded using the METAVIR system (scores 0 to 4), and the results are compared to the histological images from the same patient.

The severity of liver fibrosis is highly correlated with the growth of collagen fibers. Therefore, to quantify liver fibrosis of the imaged specimens, we analyzed the collagen content in the fibrotic tissues. The previous work of Sun et al. mentions that the intensity of SHG signal from aggregated and distributed collagen can be used to examine the extent of liver fibrosis in animal specimens.[5] In this work, we apply the aggregated and total collagen (aggregated and dispersed collagen) fibers as indicators for grading human liver fibrosis. The ratio of the total collagen area to total specimen area (TC-ratio) and area of aggregated collagen to total specimen area (AC-ratio) are determined.

For the analysis of total collagen area, the pixel numbers of the SHG image [Fig. 1(a)] having intensity above the threshold value are counted as the total collagen area. Since the intensity and distribution of aggregated collagen (black arrow) is much higher and denser than those of dispersed collagen (white arrow), we applied a 3-pixel-wide boxcar average to smooth out the dispersed collagen in the SHG images. The mean intensity of one random-selected region without aggregated collagen in the smoothed SHG image was measured as the threshold value. Then, the aggregated collagen area was isolated from the smoothed SHG image by setting this threshold value. The pixel numbers above the threshold value represent the aggregated collagen area.

3 Results

3.1 Optical Biopsy of Liver Fibrosis

The METAVIR scoring of liver fibrosis is determined by the fibrous expansion of the portal tract.[1] The portal tract is a component of the hepatic lobule and is composed of the hepatic artery, hepatic portal vein, bile duct, and lymphatic vessels. Shown in Fig. 2 and Fig. 3 are representative MAF and SHG images of liver fibrosis tissues that show morphological features corresponding to METAVIR grades 0 to 4, respectively. Histological images obtained using Masson's trichrome stains are also shown for comparison. Since we used frozen sections for multiphoton imaging, histological comparison is made by identifying similar features in Masson's trichrome–prepared specimens from an adjacent section of the tissue specimen.

Shown in Fig. 2(a) is the large-area, multiphoton image of a grade 0 METAVIR tissue, and the histological comparison is shown in Fig. 2(b). The selected region of interest (dashed frame) is shown in Fig. 2(c) as a magnified view of the portal tract surrounded by second-harmonic generating collagen fibers (yellow arrow). In addition, since hepatocyte nuclei (white arrow) lack autofluorescence, individual hepatocytes
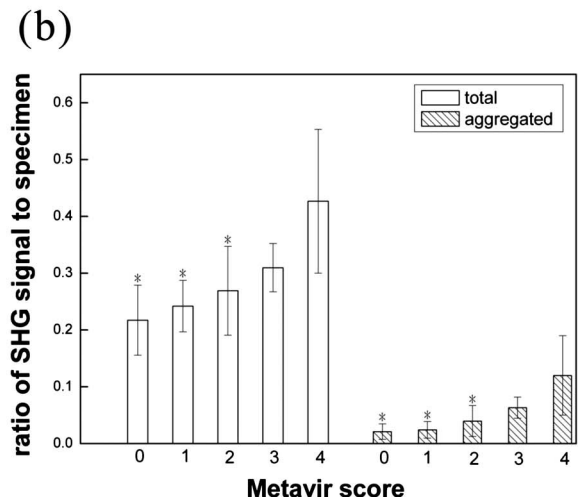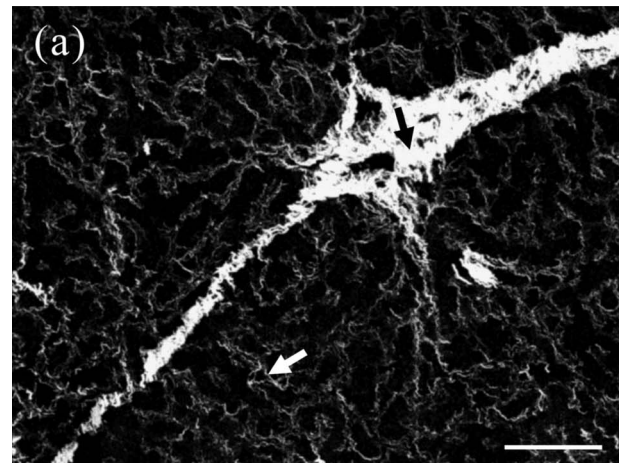

Fig. 1 (a) SHG imaging shows the distinction between aggregated (black arrow) and dispersed collagen (white arrow). Scale bar is 100 μm. (b) Relationship between AC-ratios, TC-ratios, and METAVIR grades. The specimen numbers from METAVIR scores of 0 to 4 are 5, 3, 5, 7, and 5, respectively. *; Both AC-ratios and TC-ratios of METAVIR score 0; 1 and 2 have significant difference from those of METAVIR score 4.

can be identified by round regions void of MAF surrounded by autofluorescent cytoplasm (color online only). Similar features are found in the histological image [Fig. 2(d)]. Note that in the Masson's trichrome–prepared specimen, the blue pseudo color represents the collagen fibers (yellow arrow), purple is the cytoplasm, and dark spots (white arrow) indicate positions of hepatocyte nuclei (color online only). Therefore, for collagen fibrosis identification, imaging with the spectrally separated MAF and SHG signals can provide high-contrast, label-free images comparable to that provided by conventional histological examination. In comparison, a multiphoton image of a METAVIR grade 1 specimen is shown in Fig. 3(1a). Note that the extension of liver fibrosis (yellow arrow) from a portal tract is clearly visible. Similar features can be observed in the histological comparison in Fig. 3(1b); (arrow). For imaging of a METAVIR grade 2 specimen [Fig. 3(2)], the formation of mild fibrotic bridging between two portal tracts, the hallmark of the METAVIR grade 2 pathology, can be easily identified [Fig. 3(2a)]. Once again, histological compari-
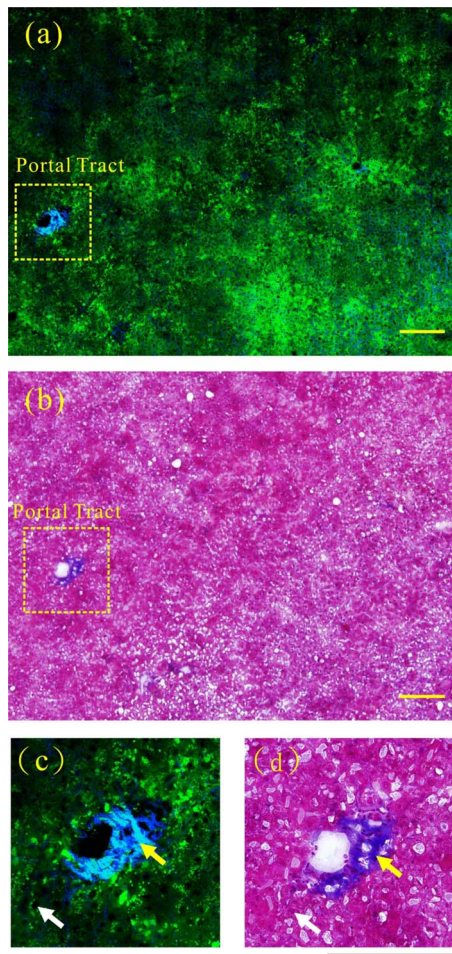
Fig. 2 Imaging of METAVIR grade 0 tissue by (a) multiphoton microscopy and (b) histological comparison. The portal tract surrounded by SHG collagen fibers (enclosed region) can be delineated. Magnified images of the selected region of interest under (c) multiphoton and (d) histological examination. The yellow arrow indicates the normal fibrous tissue of the portal tract, and the white arrow indicates the hepatocyte nucleus. Scale bar is 200 μm. (Color online only.)

Fig. 3 (1a) to (4a) Multiphoton images of METAVIR grades 1 to 4 tissue, respectively. (1b) to (4b) The corresponding histological comparison for the images shown in (a). In the METAVIR grade 1 tissue, fibrotic collagen emanating from the portal tract (enclosed region) starts to appear, while in the METAVIR grade 2 tissue, mild bridging fibrosis is evident. In the METAVIR grade 3 tissue, marked bridging fibrosis (dashed lines) between adjacent portal tracks is visible, and in the METAVIR grade 4 tissue, formation of a cirrhotic nodule is evident. All scale bars are 200 μm.

son of the METAVIR grade 2 tissue with the multiphoton results identifies similar morphological features. In multiphoton imaging of a METAVIR grade 3 specimen [Fig. 3(3a)], marked bridging fibrosis showing thick fibrotic bands is evident (dashed line). The same feature can be seen in the histological comparison [Fig. 3(3b)]. Last, for imaging of the representative grade 4 METAVIR tissue [Fig. 3(4)], the multiphoton imaging modality and the histological comparison show the enclosing of fibrotic collagen tissues and the formation of the cirrhotic nodule.

The results of liver fibrosis quantification analysis show that the TC-ratio and AC-ratio increase with the METAVIR scores [Fig. 1(b)]. The relationship between METAVIR grades and the fibrotic collagen content is summarized in Table 1. Both Fig. 1(b) and Table 1 show that the growth of fibrotic collagen in human liver increases with the severity of the METAVIR grades and that the increases of AC- and TC-ratios are nonlinear with METAVIR scores. For example, the AC-ratio increased threefold between METAVIR 3 and 0 specimens, while the same ratio increased by 5.71-fold between
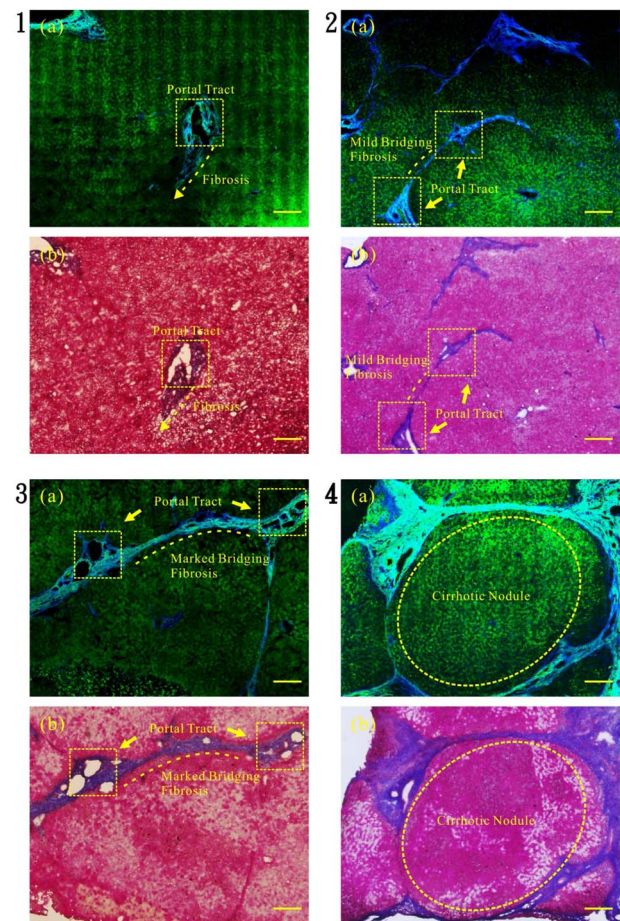
METAVIR 4 and 0 specimens. The statistical significance of the quantification of liver fibrosis was assessed by a one-way ANOVA analysis of variance and subsequent *post hoc* test using Bonferroni's Multiple Comparison Test. With $P < 0.05$ considered to be statistically significant, our analysis showed that both AC- and TC-ratios of METAVIR scores 0, 1, and 2 are significantly different from those of METAVIR score 4. Although the AC- and TC-ratios show increasing trends from METAVIR scores 0 to 3, the ratios cannot statistically differentiate between samples with those scores.

4 Conclusion

In this work, we have demonstrated the application of multiphoton and second-harmonic generation microscopy for the label-free imaging and diagnosis of *ex vivo* liver fibrosis specimens with METAVIR grades of 0 to 4. Key morphological features of differently graded liver fibrosis can be identified without extrinsic labeling. In addition, we showed that the increase of fibrotic collagen is nonlinear with the

Table 1 Relationship between differently graded METAVIR liver fibrosis specimens, TC-ratios, and AC-ratios.

METAVIR score	0	1	2	3	4
Specimen number	5	3	5	7	5
TC-ratio	0.217	0.242	0.269	0.310	0.427
SD (TC)	0.062	0.045	0.078	0.042	0.126
AC-ratio	0.021	0.024	0.039	0.063	0.120
SD (AC)	0.013	0.015	0.027	0.018	0.070

METAVIR grades. Clinically, our method can be used as a rapid, label-free, optical biopsy tool for diagnosing liver fibrosis specimens without histological preparations such as the use of Masson's trichrome staining. The spectrally distinct MAF and SHG signals can provide high-contrast tissue characterization. Furthermore, SHG signal analysis can be used to quantify the amount of fibrotic collagen and can provide an objective determination of collagen content in liver fibrosis tissues. From the result of the statistical analysis, our quantification approach could be used to discriminate normal and METAVIR score 4 liver fibrosis tissues. Further discrimination between tissues with METAVIR scores 1, 2, and 3 would likely require morphometric analysis in addition to SHG intensity analysis. Last, since multiphoton microscopy has been demonstrated to be feasible in the *in vivo* investigation of liver disease in animal models,[19,20] additional development using endoscopic techniques would enable multiphoton microscopy to become a real-time diagnostic tool for the clinical evaluation of liver fibrosis.[24]

References

1. T. Poynard, P. Bedossa, and P. Opolon, "Natural history of liver fibrosis progression in patients with chronic hepatitis C. The OB-SVIRC, METAVIR, CLINIVIR, and DOSVIRC groups," *Lancet* **349**(9055), 825–832 (1997).
2. W. Denk, J. H. Strickler, and W. W. Webb, "2-photon laser scanning fluorescence microscopy," *Science* **248**(4951), 73–76 (1990).
3. P. T. C. So, C. Y. Dong, B. R. Masters, and K. M. Berland, "Two-photon excitation fluorescence microscopy," *Annu. Rev. Biomed. Eng.* **2**, 399–429 (2000).
4. P. J. Su, W. L. Chen, J. B. Hong, T. H. Li, R. J. Wu, C. K. Chou, S. J. Chen, C. Hu, S. J. Lin, and C. Y. Dong, "Discrimination of collagen in normal and pathological skin dermis through second-order susceptibility microscopy," *Opt. Express* **17**(13), 11161–11171 (2009).
5. W. Sun, S. Chang, D. C. Tai, N. Tan, G. Xiao, H. Tang, and H. Yu, "Nonlinear optical microscopy: use of second-harmonic generation and two-photon microscopy for automated quantitative liver fibrosis studies," *J. Biomed. Opt.* **13**(6), 064010 (2008).
6. S. J. Lin, R. J. Wu, H. Y. Tan, W. Lo, W. C. Lin, T. H. Young, C. J. Hsu, J. S. Chen, S. H. Jee, and C. Y. Dong, "Evaluating cutaneous photoaging by use of multiphoton fluorescence and second-harmonic generation microscopy," *Opt. Lett.* **30**(17), 2275–2277 (2005).
7. M. J. Koehler, K. Konig, P. Elsner, R. Buckle, and M. Kaatz, "*In vivo* assessment of human skin aging by multiphoton laser scanning tomography," *Opt. Lett.* **31**(19), 2879–2881 (2006).
8. K. Konig, "Clinical multiphoton tomography," *J. Biophotonics* **1**(1), 13–23 (2008).
9. P. J. Campagnola and L. M. Loew, "Second-harmonic imaging microscopy for visualizing biomolecular arrays in cells, tissues and organisms," *Nat. Biotechnol.* **21**(11), 1356–1360 (2003).
10. W. R. Zipfel, R. M. Williams, and W. W. Webb, "Nonlinear magic: multiphoton microscopy in the biosciences," *Nat. Biotechnol.* **21**(11), 1369–1377 (2003).
11. A. Zoumi, A. Yeh, and B. J. Tromberg, "Imaging cells and extracellular matrix *in vivo* by using second-harmonic generation and two-photon excited fluorescence," *Proc. Natl. Acad. Sci. U.S.A.* **99**(17), 11014–11019 (2002).
12. S. J. Lin, S. H. Jee, C. J. Kuo, R. J. Wu, W. C. Lin, J. S. Chen, Y. H. Liao, C. J. Hsu, T. F. Tsai, Y. F. Chen, and C. Y. Dong, "Discrimination of basal cell carcinoma from normal dermal stroma by quantitative multiphoton imaging," *Opt. Lett.* **31**(18), 2756–2758 (2006).
13. H. Y. Tan, Y. Sun, W. Lo, S. J. Lin, C. H. Hsiao, Y. F. Chen, S. C. M. Huang, W. C. Lin, S. H. Jee, H. S. Yu, and C. Y. Dong, "Multiphoton fluorescence and second-harmonic generation imaging of the structural alterations in keratoconus *ex vivo*," *Invest. Ophthalmol. Visual Sci.* **47**(12), 5251–5259 (2006).
14. T. T. Le, I. M. Langohr, M. J. Locker, M. Sturek, and J. X. Cheng, "Label-free molecular imaging of atherosclerotic lesions using multimodal nonlinear optical microscopy," *J. Biomed. Opt.* **12**(5), 054007 (2007).
15. R. LaComb, O. Nadiarnykh, and P. J. Campagnola, "Quantitative second-harmonic generation imaging of the diseased state osteogenesis imperfecta: Experiment and simulation," *Biophys. J.* **94**(11), 4504–4514 (2008).
16. S. V. Plotnikov, A. M. Kenny, S. J. Walsh, B. Zubrowski, C. Joseph, V. L. Scranton, G. A. Kuchel, D. Dauser, M. S. Xu, C. C. Pilbeam, D. J. Adams, R. P. Dougherty, P. J. Campagnola, and W. A. Mohler, "Measurement of muscle disease by quantitative second-harmonic generation imaging," *J. Biomed. Opt.* **13**(4), 044018 (2008).
17. A. Uchugonova, K. Konig, R. Bueckle, A. Isemann, and G. Tempea, "Targeted transfection of stem cells with sub-20 femtosecond laser pulses," *Opt. Express* **16**(13), 9357–9364 (2008).
18. D. C. Tai, N. Tan, S. Xu, C. H. Kang, S. M. Chia, C. L. Cheng, A. Wee, C. L. Wei, A. M. Raja, G. Xiao, S. Chang, J. C. Rajapakse, P. T. So, H. H. Tang, C. S. Chen, and H. Yu, "Fibro-C-Index: comprehensive, morphology-based quantification of liver fibrosis using second-harmonic generation and two-photon microscopy," *J. Biomed. Opt.* **14**(4), 044013 (2009).
19. F. C. Li, Y. Liu, G. T. Huang, L. L. Chiou, J. H. Liang, T. L. Sun, C. Y. Dong, and H. S. Lee, "*In vivo* dynamic metabolic imaging of obstructive cholestasis in mice," *Am. J. Physiol. Gastrointest. Liver Physiol.* **296**(5), G1091–1097 (2009).
20. Y. Liu, H. C. Chen, S. M. Yang, T. L. Sun, W. Lo, L. L. Chiou, G. T. Huang, C. Y. Dong, and H. S. Lee, "Visualization of hepatobiliary excretory function by intravital multiphoton microscopy," *J. Biomed. Opt.* **12**(1), 014014 (2007).
21. T. L. Sun, Y. Liu, M. C. Sung, H. C. Chen, C. H. Yang, V. Hovhannisyan, W. C. Lin, W. L. Chen, L. L. Chiou, G. T. Huang, K. H. Kim,

P. T. C. So, H. S. Lee, and C. Y. Dong, "Label-free diagnosis of human hepatocellular carcinoma by multiphoton autofluorescence microscopy," *Appl. Phys. Lett.* **95**(19), 193703 (2009).

22. H. S. Lee, Y. Liu, H. C. Chen, L. L. Chiou, G. T. Huang, W. Lo, and C. Y. Dong, "Optical biopsy of liver fibrosis by use of multiphoton microscopy," *Opt. Lett.* **29**(22), 2614–2616 (2004).

23. V. A. Hovhannisyan, P. J. Su, Y. F. Chen, and C. Y. Dong, "Image heterogeneity correction in large-area, three-dimensional multiphoton microscopy," *Opt. Express* **16**(7), 5107–5117 (2008).

24. W. Piyawattanametha, R. P. J. Barretto, T. H. Ko, B. A. Flusberg, E. D. Cocker, H. J. Ra, D. S. Lee, O. Solgaard, and M. J. Schnitzer, "Fast-scanning two-photon fluorescence imaging based on a micro-electromechanical systems two-dimensional scanning mirror," *Opt. Lett.* **31**(13), 2018–2020 (2006).